

# Learning Uncertainty Parameters for Tactical Conflict Resolution

Sarah Degaugue, Jean-Baptiste Gotteland, Nicolas Durand

ENACLab/OPTIM  
7 av. Édouard Belin  
31055 Toulouse Cedex, France  
sarah.degaugue@alumni.enac.fr  
gottelan,durand@recherche.enac.fr

*Air Traffic Control, Conflict Detection, Uncertainties, Trajectory Prediction*

*Abstract—*

Assisting air traffic controllers in their deconfliction task is challenging. A five nautical mile separation standard in the horizontal plane and one thousand feet vertically are required in the upper airspace between aircraft. However, air traffic controllers generally need to take extra margins in their mental process. These margins can impact efficiency and capacity but are essential to safely manage the evolving traffic situations. It is necessary to model uncertainties on controllers trajectories predictions in order to design assistance tools that can mimic their perception of conflict risk. This article models uncertainties on the speed prediction, pilots reaction times when a maneuver is started or ended, and heading change accuracy. A method is proposed to estimate these values on deconflicted trajectories benchmarks. First we apply our method to benchmarks that were artificially created with an automatic solver calibrated with specific known uncertainty parameters. We show that the uncertainty on speed prediction, maneuver start time and heading change can be retrieved afterwards with a good accuracy. Then we apply our method to benchmarks of conflicts solved by qualified air traffic controllers. The method works but the quality of the results is questionable because of the small data size and the big variability in the air traffic controllers decisions.

## I. INTRODUCTION

Air traffic controllers still have very few tools to detect and solve conflicts. Many attempts have been made to ease their task in the past. The major issue controllers have to face is the lack of accuracy in trajectory prediction. Because they only have a partial control on the pilots reaction and trajectory change, they need to anticipate maneuvers and give enough margins to trajectory modifications. As long as we keep the controller in the loop of conflict detection and resolution, we need to take into account this factor. Any tool that aims at helping controllers in conflict detection must take into account uncertainties in trajectory prediction. If too much uncertainty is added to the detection, the controller will find the tool useless, sometimes bothering for situations that are not an issue. If the uncertainties are underestimated, air traffic controllers may feel unsafe because they might keep an eye on situations that are not detected by the tool. In this article, we present a model of uncertainty that is related to the behaviour of pilots and controllers and we try to calibrate the uncertainty parameters

with traffic situations solved by humans. Therefore we first test our model on artificial problems that were created using an automatic conflict solver and chosen uncertainty parameters. We show that it is possible to “guess” the uncertainty parameters used to create the maneuvers. We then use real resolution data collected on a benchmark of two and three aircraft conflicts solved by a cohort of 17 qualified air traffic controllers of the Reims Control Center to test our uncertainty model.

Conflict detection and resolution require much of Air Traffic Controller mental resources. In order to provide a tolerable level of problem complexity to air traffic controllers, the current Air Traffic Management system is divided into layers or filters, each with a decreasing time horizon. Each layer is meant to reduce the complexity of the next one. There are four major layers:

- 1) Strategic (several months before), ASM (Air Space Management): design of routes, sectors and procedures
- 2) (Pre-)Tactical (a few days to a few hours before), ATFM (Air Traffic Flow Management): control centers open schedules and define hourly capacities of each open sectors (or groups of sectors). To respect these capacity constraints, the NMOC (Network Manager Operations Center) computes and updates flow regulations and reroutings according to the posted flight plans and resulting workload excess.
- 3) Real time (5/10 minutes), tactical control: surveillance, coordination with adjacent centers, conflict resolution by various simple maneuvers (heading, flight level, speed) transmitted to the pilots.
- 4) Emergency (less than 5 minutes), safety nets: ground-based (Short Term Conflict Alert, Minimum Safety Altitude Warning) and airborne (Traffic Alert and Collision Avoidance System, Ground Proximity Warning System).

Our research focuses on the real time level. In France, like in many countries, air traffic controllers are trained to detect conflicts using a 2D horizontal visualization of the traffic. Aircraft are represented by plots and past positions of the aircraft are represented by a comet. The speed vector is materialized by a line segment representing 3,6 or 9 minutes of flight. This line segment helps the air traffic controller project future positions of the aircraft to detect potential conflicts.

Controllers can also, on demand, measure distances between points to check minimum separations, but this information is not automatically shown on the screen. There have been many attempts to organize the controller's work or assist the conflict detection task. Short Term Conflict Alert (STCA) tools are also progressively introduced in En-Route controller displays in order to ease the conflict detection but their reliability is often questioned depending on how the trajectory prediction is performed. This shows that uncertainty management plays a key role in air traffic control. [1] recently proposed a field study exploring sources of uncertainties and management strategies adopted by controllers. In the trajectory prediction, some uncertainties are constant, some other uncertainties grow with time. Corver et al recommend that controllers should be able to understand how alerts are designed, how prediction tools work and how the system is flexible for acknowledging increasing uncertainties.

First research experiments on controller assistance tools were carried out in the 1990s. In Europe, HIPS [2], [3] the Highly Interactive Problem Solver was issued from ARC2000 [4]. HIPS offered a representation of the conflict zones, called no-go-zones, in an interactive way for a chosen aircraft, knowing the intent of the other aircraft and taking into account uncertainties. An optimal maneuver time could thus be defined, but the uncertainty modeling was not detailed in the articles. The concept was more recently redefined in the Solution Space Based Diagram [5] to deal with 4D Trajectory Management. [6] compare different conflict prediction models taking into account uncertainties. They explain that uncertainty model adopted by HIPS uses geometric approach: Aircraft are modeled by ellipses and the conflict predictor compares the distance between ellipses and the separation standard. The size of the ellipse grows with time in the speed direction. This models uncertainties on aircraft speeds. Bakker and Blom compare on different scenarios the result of the geometric conflict predictor and the probabilistic model used by [7] and later adopted by [8] in the American project URET (User Request Evaluation Tool). They also introduce a third conflict predictor based on a collision risk approach. The challenge of any conflict predictor is to detect every conflict without overestimating potential conflict that will not lead to effective separation loss.

In the US, [7] introduced a conflict predictor in the 90s that was then used by [8] in URET. The model is much more technically advanced than the geometric approach. It can display conflict probabilities in complex situations. The conflict probe models trajectory prediction with gaussian distributions, calibrated on observed data. Very few details are given in Erzberger's publications on how the uncertainties were adjusted. Furthermore these uncertainties modeled aircraft future position distribution and did not try to model air traffic controllers behaviour. The conflict probe was used by [9] as a tool to assist controllers in the conflict detection task. [10] describe complex experiments done in 2008 to check how new displays of conflicts and an interactive conflict solver can help controllers deal with 3 times the current traffic. In [11], bad weather conditions and time constraints are added to check the robustness of the automated solver tool.

Besides assistance tools, much research has been done on automatic conflict resolution in the last 30 years [12], [13], [14], [15], [16], [17], [18], [19], [20]. Complex conflict situations can now be handled by automatic solvers. Hypotheses used by researchers to model the trajectories and uncertainties are generally not realistic enough to imagine a usable application, but even in the most realistic models using simple maneuvers [12], [20], the solutions found by automatic solvers have never really been compared to real situations.

None of the cited research try to model the air traffic controller uncertainty management. In this article we model air traffic controller uncertainties and introduce a method able to calibrate this model. We first detail the air traffic controller uncertainty model used in part II. Then we use an automatic solver to optimize resolutions using nominal uncertainty parameters on a benchmark of random conflicts (part III). We show in part IV that we can learn the uncertainty parameters used with a benchmark of resolutions using these parameters. Part V show the uncertainty parameters found with this approach on a benchmark of resolutions performed by qualified air traffic controllers of the Reims Control Center.

## II. AIR TRAFFIC CONTROLLER UNCERTAINTY MODEL

Air traffic controllers need to anticipate aircraft positions taking into account several uncertainties. These uncertainties have been taken into account in previous work [20], [21] but we never managed to give realistic values to the different parameters defined. In [20] we introduced the model in the horizontal plane. In [21] we added the vertical dimension that we do not consider in this article, but will add in future work.

### A. Maneuvers

We discretize time into steps of duration  $\tau$  to describe maneuvers.  $\tau$  is small enough to detect every conflict in the application. In the experiments,  $\tau = 3$  s because two facing aircraft flying at 600 kt (maximal speed) get only 1 NM closer every 3 s, so we will never miss any conflict with such a small  $\tau$  value ([22] discusses the topic).

In our trajectory model, maneuvers are heading changes of  $\alpha$  degrees, at starting time  $t_0$ , until ending time  $t_1$ . Heading changes  $\alpha$  can take different values that are discretized by steps of 5 degrees, in order to comply with air traffic controllers practice.  $\alpha$  is relative to the current heading. Figure 1 summarizes a current Air Traffic Control maneuver which can easily be implemented by pilots and current FMS technologies (cf. [23]).

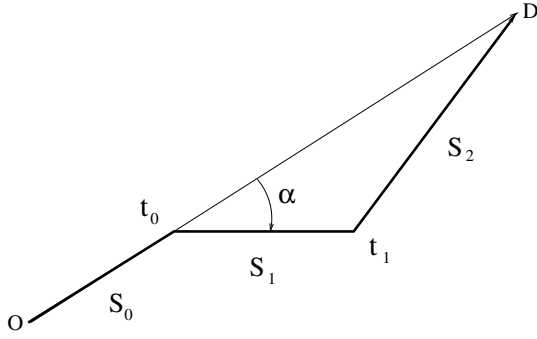
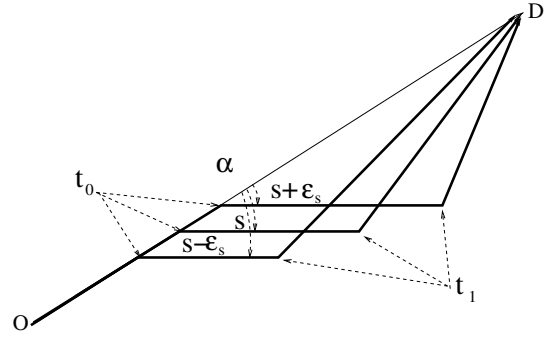
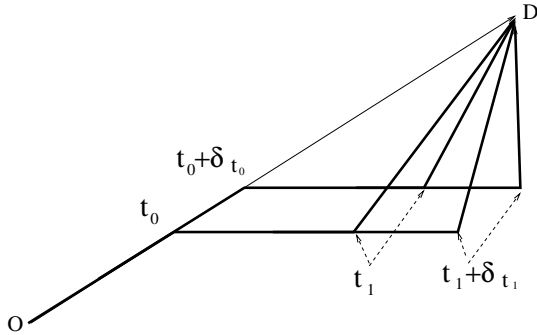
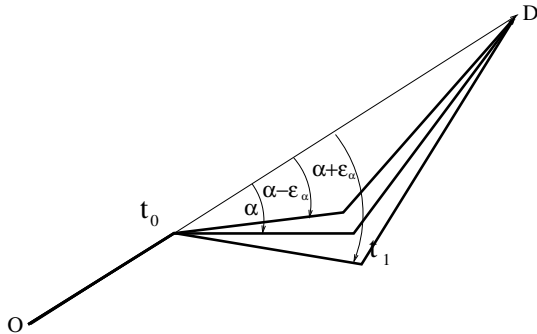


Fig. 1: Maneuver model.

Fig. 4: Speed uncertainty:  $\varepsilon_s$ 

We model four different sources of uncertainties:

- When pilots get maneuver orders, they can react more or less quickly. An uncertainty  $\delta_{t_0} \in [0, \Delta_{t_0}]$  representing the maximum reaction time for beginning a maneuver is associated with time  $t_0$  (figure 2);
- An uncertainty  $\delta_{t_1} \in [0, \Delta_{t_1}]$  representing the maximum reaction time for resuming the initial route (i.e. heading to the next beacon of the route) is associated with time  $t_1$  (figure 2);
- An uncertainty  $\varepsilon_\alpha \in [-E_{\alpha_{Max}}, E_{\alpha_{Max}}]$  is also associated with the heading change angle  $\alpha$  (figure 3);
- Aircraft speeds are also subject to a  $\varepsilon_s \in [-E_{s_{Max}}, E_{s_{Max}}]$  error such that future positions of aircraft are spread over a range which grows with time (figure 4);

Fig. 2: Pilot execution time uncertainties:  $\delta_{t_0}$  and  $\delta_{t_1}$  model.Fig. 3: Maneuver angle uncertainty:  $\varepsilon_\alpha$  model.

## B. Handling Uncertainties

We define three different states for a maneuvered aircraft (see figure 1) depending on the fact that it has not started its maneuver (State  $S_0$ ), it has started its maneuver (State  $S_1$ ), or it has ended its maneuver (State  $S_2$ ). In the prediction, the initial position of an aircraft is a point (the current known position of the aircraft). At each time step the position of the aircraft is recalculated according to the previously defined uncertainties. Because of the speed uncertainty, an aircraft position at time  $t$  can lead to different positions at time  $t + \tau$ . If a maneuver is decided at time  $t_0$  and the current time  $t_{cur} \in [t_0, t_0 + \Delta_{t_0}]$ , the next position can either take into account the maneuver or not, which creates two different possible positions of the aircraft, with different status. In one case the aircraft is still not maneuvered, and will remain in state  $S_0$ . In the second case the aircraft has started its maneuver and switches to state  $S_1$ . The same process occurs when the current time  $t_{cur} \in [t_1, t_1 + \Delta_{t_1}]$ . Each aircraft position is described at every time step  $\tau$  (i.e.  $0, \tau, 2\tau, 3\tau \dots$ ) by three convex hulls corresponding to the three possible states ( $S_0, S_1$  or  $S_2$ ) of the aircraft. Only the extreme points of the convex hulls are used to define the new possible aircraft positions. This prevents the trajectory prediction from becoming too much time consuming. Convex hulls are computed with Graham's algorithm [24].

Figure 5 gives an example of maneuver with the different states. In red, the aircraft has not started any maneuver. In green, the aircraft has changed its heading, and in blue, it is heading back to the next point on its route ( $D$ ). The gray line gives the convex hull of the three states. The conflicts will then be detected between such convex hulls by computing their relative distance.

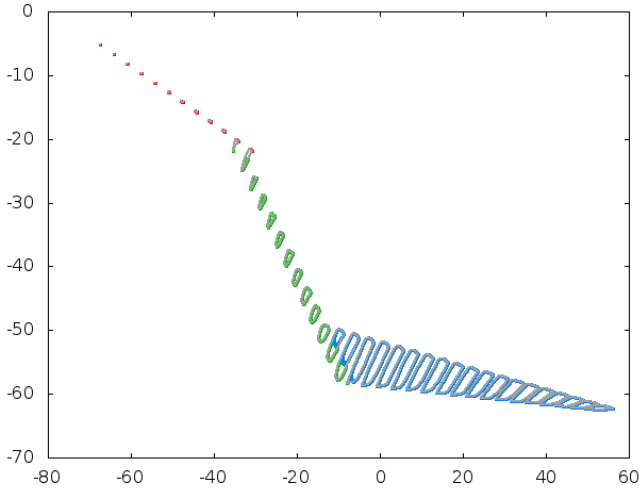


Fig. 5: An example of trajectory prediction. Red, green and blue correspond respectively to states  $S_0$ ,  $S_1$  and  $S_2$ ; Grey parts represent the convex hulls.

Any traffic simulator using any kind of uncertainty hypothesis can be adapted to build the trajectory prediction for the aircraft and for the maneuver options. It is also possible to have different uncertainties for different aircraft. We can also use different maneuver options if necessary. The convex hull prevents the detection algorithm from missing a potential conflict according to the chosen uncertainties.

This approach can easily be generalized to the third dimension (vertical plane), taking into account uncertainties on the climbing rate of the aircraft. Convex 3D-volumes can thus be defined and conflicts detected according to the horizontal and vertical distance between them.

### III. NOMINAL BENCHMARK USING AN AUTOMATIC SOLVER

In this section, we detail how we build nominal benchmarks that will be used in section IV to evaluate the uncertainty parameters. Because we know the uncertainties used to build the nominal benchmarks, we will be able to check how our learning process can recover these parameters.

#### A. Building a Nominal Benchmark

Before calibrating the uncertainty model using a benchmark of conflicts solved by air traffic controllers, we want to validate our approach on “nominal benchmarks” on which we know what uncertainties were used. We want to make sure the calibration gives us the values of the uncertainties that were used to build the benchmark.

To build a nominal benchmark we use a conflict generator and solve conflicts in a centralized way using an evolutionary algorithm (EA) that predicts trajectories with the uncertainty model described in section II. The EA used is similar to those described in [12] and [25]. It finds optimal maneuvers  $(t_0, t_1, \alpha)$  for each aircraft of a scenario with the uncertainty model. The EA presented in this section is different from the EA used in section IV. It is used to find conflict free

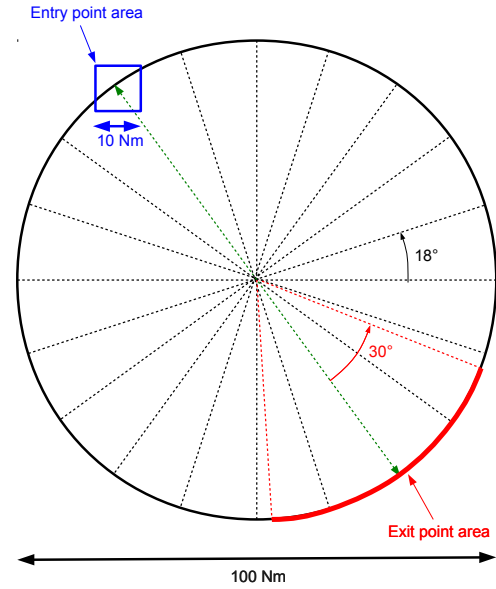


Fig. 6: Generation of random traffic situations.

trajectories to build nominal benchmarks. The EA creates a population of 50 random solutions in which each aircraft is given no more than one maneuver. It first tries to find conflict free solutions without trying to optimize maneuvers and then spends an extra 20 generations minimizing the number of maneuvers and finally minimizing the generated delays. 40% of each population is crossed, 40% of each population is muted. It uses  $\sigma$  truncation scaling and a simple sharing process that divides the fitness of solutions that share the same characteristics by their occurrence numbers: two solutions share the same characteristics if they turn right or left or keep straight the same aircraft. The EA returns a near optimal solution for each scenario. For scenarios with two aircraft, the EA generally solves the conflict with one maneuver.

#### B. Exercise generation

In order to generate random traffic scenarios with different types of conflicts between aircraft, we consider a circular sector with a diameter of 100 nautical miles (about 15 minutes of flying time for an aircraft), with 20 possible entry points regularly positioned on its circumference (see figure 6). With these orders of magnitude, the distance between two neighboring entry points is over 15 nautical miles (which is three times greater than the minimal separation distance between aircraft).

For the nominal tests, the number of aircraft in the traffic situations is set to 2. Each aircraft is randomly assigned:

- a nominal speed, between 370 and 550 knots;
- its own entry point, in a rectangular area of 10 nautical miles around one of the sector’s entry points;
- an exit point on the opposite side of the sector, in a slice extending by plus or minus 30 degrees around the opposite point on the circle.

Initially, each aircraft flies directly from its entry point to its exit point.

In order to build conflict scenarios and avoid unmanageable traffic situations, the following constraints were required additionally (situations not respecting these constraints were discarded):

- A conflict must happen considering the uncertainty chosen;
- A minimal duration of 3 minutes was required before the first conflict happens.

Using this process, we generate nominal benchmarks  $\Omega_{\varepsilon_s, \delta_{t_0}, \delta_{t_1}, \varepsilon_\alpha}$  of 40 scenarios using uncertainties  $\varepsilon_s$ ,  $\delta_{t_0}$ ,  $\delta_{t_1}$  and  $\varepsilon_\alpha$ . These scenarios will be used in section IV in order to check that uncertainties can be retrieved.

#### IV. LEARNING THE NOMINAL UNCERTAINTY PARAMETERS

In order to calibrate the uncertainty model described in section II, we adjust uncertainties on the deconflicted trajectories in order to reach a minimal distance as close as possible to 5 nautical miles between the uncertainty volumes around the trajectories. Therefore, we define a function  $d_\omega(\varepsilon_s, \delta_{t_0}, \delta_{t_1}, \varepsilon_\alpha)$  that calculates the minimum distance between trajectories, given the uncertainty parameters  $(\varepsilon_s, \delta_{t_0}, \delta_{t_1}, \varepsilon_\alpha)$ , on the scenario  $\omega$ . Function  $d_\omega$  can be applied to a benchmark  $\Omega$  of deconflicted aircraft scenarios and our objective is to minimize:

$$D_\Omega(\varepsilon_s, \delta_{t_0}, \delta_{t_1}, \varepsilon_\alpha) = \sum_{\omega \in \Omega} [d_\omega(\varepsilon_s, \delta_{t_0}, \delta_{t_1}, \varepsilon_\alpha) - norm_d]^2 \quad (1)$$

For the benchmark  $\Omega$ , the minimum of  $D_\Omega$  for a benchmark returns the uncertainty parameters for which resolutions comply *the most* with  $norm_d$  when these uncertainties are applied and thus calibrates the values of these uncertainties on the benchmark.

Nominal scenarios were created as described in section III. For each nominal benchmark  $\Omega_{\varepsilon_s, \delta_{t_0}, \delta_{t_1}, \varepsilon_\alpha}$  of 40 scenarios, the same uncertainties have been chosen and the resulting data are aircraft trajectories before and after resolution. Before resolution, we save the trajectory containing the origin and the destination of each aircraft. After resolution, the new trajectories of the deviated aircraft are added.

In order to optimize the four uncertainty values, we minimize the function  $D_\Omega$  defined in (1) on benchmark  $\Omega$ : we want to find the uncertainties  $\varepsilon_s$ ,  $\delta_{t_0}$ ,  $\delta_{t_1}$ , and  $\varepsilon_\alpha$  that were used to create the benchmark in order to validate the method.

Because the minimization criteria is the result of simulations, we can only use optimization techniques that do not require any analytical expression of the minimization criteria. Furthermore, we have no idea of the regularity of the minimization criteria. We decided to use an evolutionary algorithm to minimize  $D_\Omega$  because it is robust to premature convergence. In addition, an evolutionary algorithm as described in [12] is generally more robust to the multimodal characteristics of our problem.

##### A. Evolutionary algorithm

We decided to use a simple evolutionary algorithm to find the four parameters  $\varepsilon_s$ ,  $\delta_{t_0}$ ,  $\delta_{t_1}$  and  $\varepsilon_\alpha$  that minimize  $D_\Omega$

on a benchmark of solved scenarios  $\Omega$ . The elements in our population correspond to a data type with four variables:

- The velocity uncertainty (between 0 and 20 %)  $\varepsilon_s \in [0; 0.2]$ ;
- The pilot answer uncertainty at the beginning of the maneuver  $\delta_{t_0} \in [0; 60]$ ;
- The pilot answer uncertainty at the end of the maneuver  $\delta_{t_1} \in [0; 60]$ ;
- The heading uncertainty during the maneuver  $\varepsilon_\alpha \in [0; 10]$ .

Because the EA seeks for a maximum, we used the following fitness function to minimize the difference between  $d_\omega$  and  $norm_d$  for each  $\omega \in \Omega$ :

$$f(\varepsilon_s, \delta_{t_0}, \delta_{t_1}, \varepsilon_\alpha) = \frac{|\Omega|}{|\Omega| + D_\Omega(\varepsilon_s, \delta_{t_0}, \delta_{t_1}, \varepsilon_\alpha)} \quad (2)$$

A population of 20 elements is randomly generated at the beginning of the EA. The population is rather small because we only optimize four variables and the fitness evaluation is rather long (it is the result of the 40 scenarios simulation for each population element). For each individual of a generation, its uncertainties are taken into account when applying the aircraft maneuvers for each scenario and its fitness is then calculated. The EA is stopped after 300 generations.

We decided to cross 20% of the population using an arithmetic crossover and to mutate 30% of the population by randomly choosing one of the four uncertainty variables and adding a random noise to it. The noise is randomly chosen in an interval centered in 0 of magnitude 10% of the corresponding uncertainty domain. A sharing process is used to avoid premature convergence. The euclidean distance is used for the sharing process. The different parameters used (percentage of crossover, mutation, type of mutation) were adjusted empirically by testing different options.

##### B. Results on nominal benchmarks

We first validate our approach by using a benchmark for which we know the uncertainties used. We want to make sure that the EA gives us values that are close to uncertainties used to build the benchmark. On a first benchmark using uncertainties  $(\varepsilon_s = 0.1, \delta_{t_0} = 30, \delta_{t_1} = 30, \varepsilon_\alpha = 5)$  the EA gives us  $(\varepsilon_s = 0.1, \delta_{t_0} = 30, \delta_{t_1} = 48, \varepsilon_\alpha = 5.8)$ . Uncertainties found for the speed, for  $t_0$  and for  $\alpha$  are close to the one used to create the benchmark. Uncertainty on  $t_1$  is very different. In order to understand why, we show in figure 7 the behavior of the fitness function when we assign three uncertainties to their optimal values and allow the fourth uncertainty to vary.

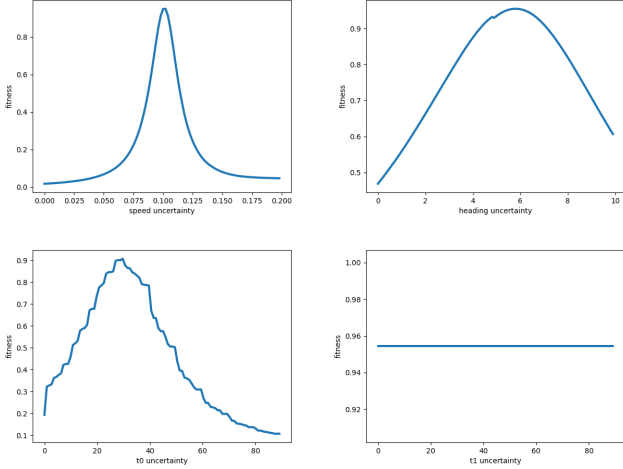


Fig. 7: Fitness as a function of the uncertainty parameters

Figure 7 details the fitness curves according to the four uncertainties: 10 % for the speed, 30 seconds for  $t_0$ , 48 seconds for  $t_1$  and 5.8 degrees for the heading.

The uncertainties related to the speed, to the maneuver start and to the heading show a peak of fitness consistent with the value of the expected uncertainty. We remain slightly above 5 degrees, but this could be due to the fact that the automatic solver used in section III discretizes angles by steps of 5 degrees and keeps a minimum of 5 nautical miles between aircraft.

The slightly chaotic aspect of the fitness curve as a function of the  $t_0$  uncertainty justifies the choice of an evolutionary algorithm as local maximums are present.

The fitness curve as a function of  $t_1$  is flat, which means that our benchmark involving only two aircraft scenarios don't permit to detect uncertainties due to the end of maneuver execution. This can be explained by the fact that if pilots do not end their maneuver once the conflict is over, it does not create any new conflict (This is particularly true for two aircraft conflicts).

For this benchmark, figure 8 illustrates the minimal distances between aircraft (after resolution), as a function of their initial headings difference, measured with and without uncertainties.

Each point represents a particular scenario that has been created and previously solved by our automatic solver. With the uncertainties found by the EA (red points), the minimum distances are close to 5 nautical miles as expected.

In table I, we give results on different nominal benchmarks built with 9 different combinations of uncertainties. The four first columns give the uncertainties used to build the 9 different benchmarks. The four next columns give the uncertainties found by the EA. The fitness columns compare the fitness expected with the original uncertainties to the optimized fitness.  $|d_\omega - norm_d|$  for all  $\omega \in \Omega$  represents the error of the model. The last two columns give the mean and standard deviation of  $|d_\omega - norm_d|$ .

The optimal expected fitness is generally lower than the obtained fitness because the automatic solver stays above the 5 nautical miles separation. In the optimization process,  $norm_d$

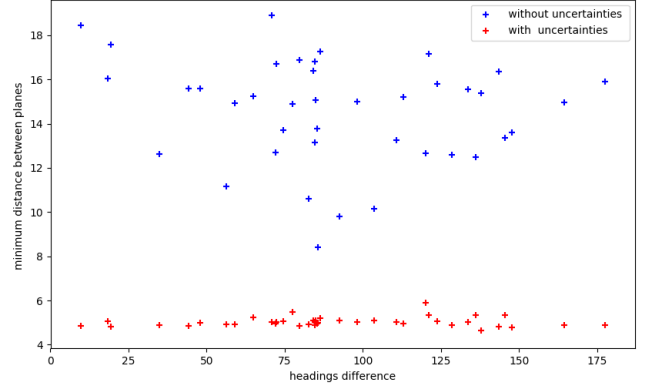


Fig. 8: Nominal case : Minimum distance between uncertainty volumes (**with uncertainties**) or between nominal trajectories (**without uncertainties**)

should probably be set to a higher value to improve the results. First trials done with  $\sqrt{28}$  tend to confirm this hypothesis. For the seek of clarity of the paper, we do not develop this option in this article.

In table I the speed, maneuver start, and heading change uncertainties are generally very close to the expected values, even for extreme uncertainty values. The error of the model is a little higher for cases where the uncertainties are very low or very high.

We introduced this first step using nominal benchmarks to validate our approach. Results show that the method can find three of the four uncertainty values with a good accuracy: the speed, maneuver start, and heading change uncertainties. To find the uncertainty on the end of maneuver, we should probably use more complex scenarios or maybe refine the optimization criteria. In the next section we apply this approach on conflicts solved by qualified air traffic controllers.

## V. RESULTS ON EXPERIMENTS WITH AIR TRAFFIC CONTROLLERS

### A. Results on two aircraft benchmarks

We extracted from experiments done in the Reims Control Center presented in [26] two aircraft resolution scenarios solved by air traffic controllers. The benchmark includes 46 scenarios involving 8 different conflicts with 2 levelled aircraft solved by 17 air traffic controllers. We kept the scenarios for which no more than one maneuver per aircraft had been given, and for which the conflict was solved.

The EA presented in section IV estimates the speed uncertainty on close to 0,8%, the time uncertainty  $t_0$  close to 145 seconds and the heading uncertainty close to 1.5 degrees (The time bound of 60 seconds used in the nominal benchmarks was increased because initial tests showed that is was too small). Figure 9 shows the shape of the fitness as a function of one out of the four uncertainties when the three others are assigned their optimal value. It is once again clear that the uncertainty on the end of maneuver cannot be estimated with this approach.

TABLE I: Results on nominal benchmarks

Expected uncertainties				Optimized uncertainties				Fitness		$ d_\omega - norm_d $	
s	$t_0$	$t_1$	h	s	$t_0$	$t_1$	h	exp	opt	$\nu$	$\sigma$
0.01	30.	30.	5.	0.01	30	57	7.6	0.80	0.91	0.22	0.24
0.1	30.	30.	5.	0.10	30	48	5.8	0.92	0.95	0.15	0.16
0.1	5.	30.	5.	0.10	4.3	60.	5.6	0.89	0.95	0.18	0.14
0.01	15.	15.	1.	0.01	18	4.5	1.9	0.85	0.91	0.21	0.22
0.1	30.	30.	1.	0.01	29	3.4	2.5	0.89	0.95	0.17	0.16
0.2	50.	50.	10.	0.21	50	60.	9.9	0.84	0.90	0.23	0.24
0.2	30.	30.	5.	0.20	30	8.9	6.6	0.78	0.89	0.26	0.23
0.1	30.	30.	10.	0.1	37	37	9.4	0.89	0.94	0.21	0.16
0.1	50.	30.	5.	0.10	48	27	6.0	0.91	0.96	0.16	0.15

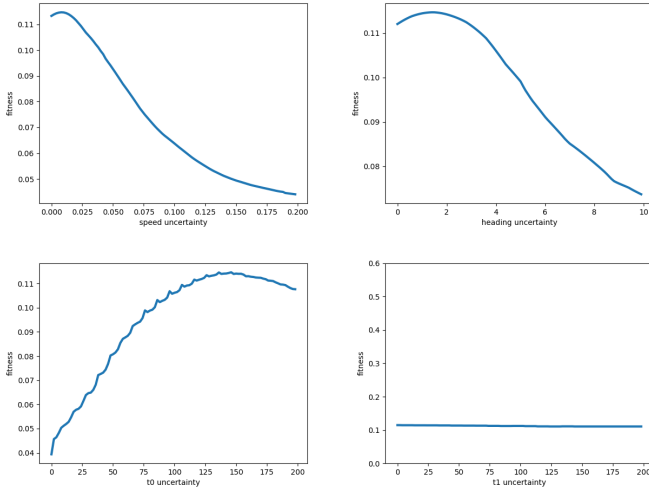


Fig. 9: Fitness as a function of the uncertainty parameters

Furthermore, the average of  $|d_\omega - norm_d|$  is approximately equal to 2.18 with a standard deviation of 1.72, consequently the model error is 10 times higher than for the nominal cases. Figure 10 illustrates the distances on these scenarios  $d_\omega$  for all  $\omega \in \Omega$  as a function of the difference between the initial headings of the aircraft with the uncertainties determined by the algorithm (in red) and without uncertainties (in blue). The cloud of red points is spread around the 5 nautical mile ordinate because we minimize  $\sum_{\Omega} (d_\omega - norm_d)^2$ . We clearly see a great variability of the decisions of the various air traffic controllers. 8 columns of points are identifiable: these are the different scenarios resolved by the controllers. Blue points represent the minimum distance between the aircraft at the end of the resolution by the controllers, without any consideration of uncertainties.

### B. Results on three aircraft benchmark

We extracted from experiments done in the Reims Control Center the three aircraft resolution scenarios solved by 17 air traffic controllers. The benchmark includes 35 different scenarios with 3 levelled aircraft. We kept the scenarios for which at most one maneuver per aircraft had been given, and for which the conflict was solved. For each maneuver of each scenario, we initialize the uncertainty half a minute before the decision was made by the air traffic controller. If

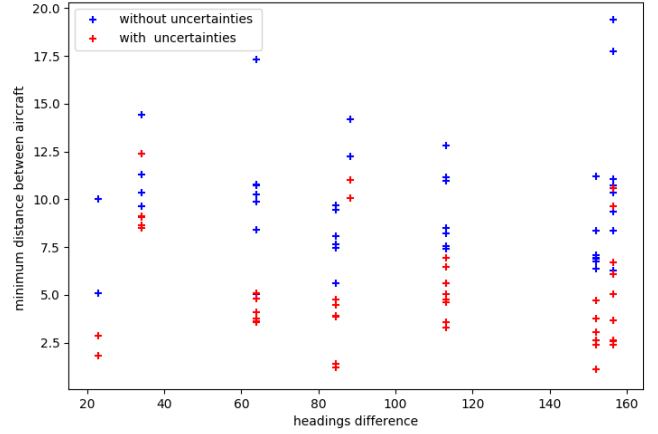


Fig. 10: Two aircraft experiments : Minimum separation distance between aircraft with and without uncertainties

two maneuver decisions are made at two different times, we duplicate the scenario in order to start the uncertainty half a minute before each maneuver and calculate  $d_\omega$  as the minimal distance between the trajectory of the maneuvered aircraft and the two other trajectories. Because we duplicate scenarios we end up with 73 scenarios.

The EA estimates the speed uncertainty close to 1.4%, the time uncertainty  $t_0$  close to 22 seconds and the heading uncertainty close to 3.9 degrees. Figure 11 shows the shape of the fitness as a function of one out of the four uncertainties when the three others are assigned their optimal value. The uncertainty on the end of maneuver still cannot be estimated with this approach.

The average of  $|d_\omega - norm_d|$  is approximately equal to 2.36 with a standard deviation of 2.1. Figure 12 illustrates the distances on these scenarios  $d_\omega$  for all  $\omega \in \Omega$  as a function of the difference between the initial headings of the aircraft with the uncertainties determined by the algorithm (in red) and without uncertainties (in blue). We clearly observe that the red points spread around the 5 nautical mile line.

### C. Discussion

1) *Two aircraft benchmark*: Several observations can be made. First, for small differences between initial headings, less controllers were able to solve conflicts. This is probably



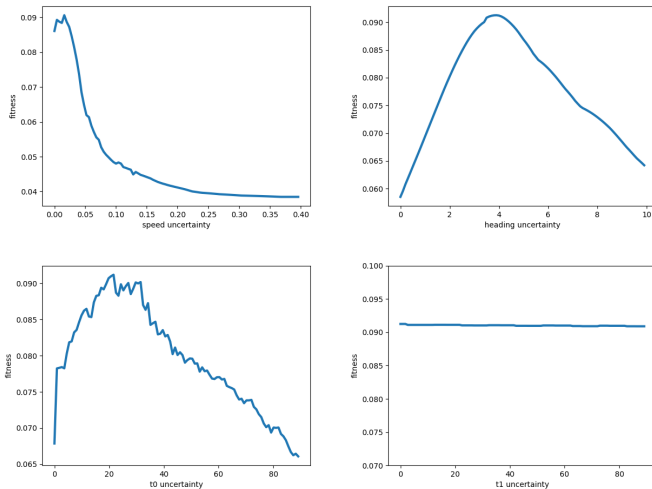


Fig. 11: Fitness as a function of the uncertainty parameters

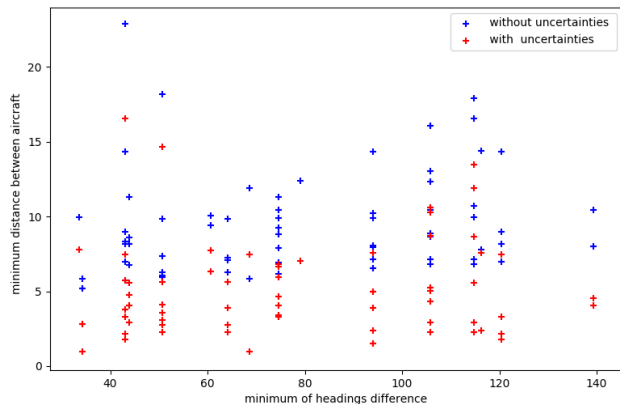


Fig. 12: Three aircraft experiments : Minimum separation distance between aircraft with and without uncertainties

due to the fact that these conflicts are more difficult to solve and need a quick decision. The number of collected scenarios on these cases is probably too small to draw conclusions.

Second, there is a big variability of controllers response to the same conflict configurations. This explains the rather high value of the model error. It is probably necessary to collect many more scenarios for a panel of different controllers to give an interpretation to these results.

Third, if confirmed on bigger data sets, these results could show that air traffic controllers may be very sensitive to the uncertainty on the pilot response (estimated to 145 s).

2) *Three aircraft benchmark*: Results on the three aircraft benchmark show a much smaller uncertainty on the pilot response (20s), which could be explained by the fact that air traffic controllers took a longer time to analyse the situation, and waited to be closer to the conflict to make a decision. These conflicts are more difficult to solve and can probably not handle big uncertainties. We are aware of the questionable reliability of these results on such a small benchmark.

## VI. CONCLUSION AND FURTHER WORK

To conclude, we introduced in this article an approach that models and estimates uncertainties on trajectories due to conflict resolution. We validated the estimation process on nominal benchmarks and showed that three out of the four uncertainties modeled could rather precisely be estimated by minimizing  $D_{\Omega}(\varepsilon_s, \delta_{t_0}, \delta_{t_1}, \varepsilon_{\alpha})$  on conflict scenarios.

We applied this approach on air traffic controllers conflict resolutions involving two and three aircraft. We showed that our model could still return values for the speed, maneuver start and heading change uncertainty but the quality of the results are not as good. The mean error remains above 2 nautical miles after applying the estimated uncertainties. This prevents from building strong conclusions on the results, even if we can make hypotheses to explain the orders of magnitude observed in the results.

Results show that we need to perform our estimation model on much bigger benchmarks. It could be interesting to individualize the estimation on each controller to see if we can observe different behaviors. We are currently working on collecting big data sets to move forward in this direction. We could also extend our model to the vertical dimension, by adding uncertainties on climbing and descending rates.

However, this paper introduces an original approach to model how air traffic controllers deal with uncertainties related to conflict resolution in a scientific manner. The goal is that future decision support tools become accepted and efficient for air traffic controllers by ensuring that the uncertainty model matches their own perception of conflict risk.

We really wanted to focus on the method in this article, which is a first step toward a stronger study of the air traffic controller uncertainty model for which more work is needed.

## REFERENCES

- [1] S. Corver and G. Grote, "Uncertainty management in enroute air traffic control: a field study exploring controller strategies and requirements for automation," *Cognition, Technology & Work*, vol. 18, pp. 541–565, Aug 2016.
- [2] D. C. Meckiff and D. P. Gibbs, "PHARE : Highly interactive problem solver," tech. rep., Eurocontrol, 1994.
- [3] A. Price and C. Meckiff, "Hips and its application to oceanic control," in *1st ATM R&D Seminar*, 1997.
- [4] G. Dean, X. Fron, W. Miller, and J. Nicolaon, "Arc2000 : An investigation into the feasibility of automatic conflict," tech. rep., Eurocontrol Experimental Center, 1995.
- [5] R. Klomp, R. Riegman, C. Borst, M. Mulder, and M. M. Van Paassen, "Solution space concept: Human-machine interface for 4d trajectory management," in *13th USA-Europe Air Traffic Management Research and Development Seminar*, 06 2019.
- [6] G. Bakker and H. Blom, "Wp1: Comparative analysis of probabilistic conflict prediction approaches in atm," tech. rep., NLR Contract Report, 2000.
- [7] H. Erzberger, "Conflict probing and resolution in the presence of errors," in *Proceedings of the 1st USA/Europe ATM R and D Seminar*, 1997.
- [8] W. C. Arthur and M. P. McLaughlin, "User request evaluation tool (uret). interfacility conflict probe performance assessment," in *Proceedings of the 2nd USA/Europe ATM R and D Seminar*, 1998.
- [9] T. Prevot, P. Lee, N. Smith, and E. Palmer, "Atc technologies for controller-managed and autonomous flight operations," in *AIAA Guidance, Navigation and Control Conference and Exhibit*, 2005.
- [10] T. Prevot, J. Homola, and J. Mercer, "Initial study of controller/automation integration for nextgen separation assurance," in *AIAA Guidance, Navigation and Control Conference and Exhibit*, 2008.



- [11] T. Prevot, J. Homola, L. Martin, and J. Mercer, "Automated air traffic control operations with weather and time-constraints," in *9th ATM R&D Seminar*, 2011.
- [12] N. Durand, J.-M. Alliot, and J. Noailles, "Automatic aircraft conflict resolution using genetic algorithms," in *Proceedings of the Symposium on Applied Computing, Philadelphia*, ACM, 1996.
- [13] J.-H. Oh, J. Shewchun, and E. Feron, "Design and analysis of conflict resolution algorithms via positive semidefinite programming [aircraft conflict resolution]," in *Decision and Control, 1997., Proceedings of the 36th IEEE Conference on*, vol. 5, pp. 4179–4185 vol.5, Dec 1997.
- [14] E. Frazzoli, Z.-H. Mao, J.-H. Oh, and E. Feron, "Resolution of conflicts involving many aircraft via semidefinite programming," *AIAA Journal of Guidance, Control and Dynamics*, vol. 24, Jan-Feb 2001.
- [15] L. Pallottino, A. Bicchi, and E. Feron, "Mixed integer programming for aircraft conflict resolution," in *AIAA Guidance Navigation and Control Conference and Exhibit*, 2001.
- [16] L. Pallottino, E. Feron, and A. Bicchi, "Conflict resolution problems for air traffic management systems solved with mixed integer programming," *Intelligent Transportation Systems, IEEE Transactions on*, vol. 3, pp. 3–11, Mar 2002.
- [17] M. A. Christodoulou and C. Kontogeorgou, "Collision avoidance in commercial aircraft free flight via neural networks and non-linear programming," *Int. J. Neural Syst.*, vol. 18, no. 5, pp. 371–387, 2008.
- [18] A. Alaeddini, H. Erzberger, and W. Dunbar, "Distributed logic-based conflict resolution of multiple aircraft in planar en-route flight," in *AIAA Guidance, Navigation and Control Conference and Exhibit*, 2011.
- [19] M. Gariel and E. Feron, "3d conflict avoidance under uncertainties," in *Digital Avionics Systems Conference, 2009. DASC '09. IEEE/AIAA 28th*, pp. 4.E.3–1–4.E.3–8, Oct 2009.
- [20] C. Allignol, N. Barnier, N. Durand, and J.-M. Alliot, "A new framework for solving en-routes conflicts," in *10th USA/Europe Air Traffic Management Research and Development Seminar*, 2013.
- [21] C. Allignol, N. Barnier, N. Durand, A. Gondran, and R. Wang, "Large Scale 3D En-Route Conflict Resolution," in *ATM Seminar, 12th USA/Europe Air Traffic Management R&D Seminar*, (Seattle, United States), June 2017.
- [22] N. Barnier and C. Allignol, "Trajectory deconfliction with constraint programming," *The Knowledge Engineering Review*, vol. 27, no. 03, pp. 291–307, 2012.
- [23] G. Granger, N. Durand, and J. Alliot, "Optimal resolution of en-route conflicts," in *4th ATM R&D Seminar*, 2001.
- [24] R. L. Graham, "An efficient algorithm for determining the convex hull of a finite planar set," in *Information Processing Letters*, 1992.
- [25] N. Durand and J.-M. Alliot, "Optimal resolution of en route conflicts," in *First ATM Seminar Europe/USA, Saclay*, 1997.
- [26] N. Durand, J.-B. Gotteland, N. Matton, L. Bortolotti, and M. Sandt, "Understanding and overcoming horizontal separation complexity in air traffic control: an expert/novice comparison," *Cognition, Technology and Work*, 2020.

**Sarah Degaugue** is a master's student in Operational Research (OR). She is currently in her last year of engineering at the École Nationale de l'Aviation Civile (ENAC).

**Jean-Baptiste Gotteland** is an assistant professor at the École Nationale de l'Aviation Civile (ENAC). He graduated from ENAC as an engineer in 1995, and received a PhD (2004) in computer science from the University of Toulouse.

**Nicolas Durand** is a professor at the École Nationale de l'Aviation Civile (ENAC). He graduated from the École Polytechnique de Paris in 1990 and from ENAC in 1992. He has been a design engineer at the Centre d'Études de la Navigation Aérienne (then DSNA/DTI R&D) from 1992 to 2008, holds a PhD in Computer Science (1996) and got his HDR (French tenure) in 2004.